Optics Communications 364 (2016) 191–194

Contents lists available at ScienceDirect

Optics Communications

journal homepage: www.elsevier.com/locate/optcom

Simultaneous measurement of refractive index and temperature based on asymmetric structures modal interference

Huihao Wang [a], Hongyun Meng [a,*], Rui Xiong [b], Qinghao Wang [a], Ben Huang [a], Xing Zhang [a], Wei Yu [a], Chunhua Tan [a], Xuguang Huang [a]

[a] Guangdong Provincial Key Laboratory of Nanophotonic Functional Materials and Devices, School for Information and Optoelectronic Science and Engineering, South China Normal University, Guangzhou 510006, PR China
[b] China Academy of Information and Communications Technology, Guangzhou 510006, PR China

ARTICLE INFO

Article history:
Received 7 September 2015
Received in revised form
25 October 2015
Accepted 7 November 2015
Available online 6 December 2015

Keywords:
Fiber sensor
Mach–Zehnder interferometer
Refractive index
Temperature

ABSTRACT

An in-line fiber sensor for simultaneous measurement of refractive index (RI) and temperature is proposed and demonstrated. The sensor head is composed of an asymmetric Mach–Zehnder interferometer (MZI), which is combining the single mode-multimode-single mode (SMS) fiber structure and a peanut-shape structure. The transmission dips of the sensor will shift as the ambient RI or temperature variation due to the phase changing. The different wavelength transmission dips formed by the cladding modes interfering with the core mode have different sensitivity responses, so the simultaneous measurement of the RI and temperature can be achieved by monitoring the wavelength shifts of the two transmission dips. The experimental results show that the sensing sensitivities of RI and temperature are −86.7434 nm/RIU and 0.0590 nm/°C in the RI range from 1.3105 to 1.3517 and temperature range from 25 °C to 85 °C, respectively. The novel sensor processes easy fabrication, low cost, and high sensitivity, making it offers high potential applications in physical, biological and chemical sensing.

1. Introduction

Fiber-based refractive index sensors have been widely used in many fields such as biochemical analysis, chemical industry and environment assessment for their numerous advantages over conventional sensors, such as small size, easy fabrication, real-time, corrosion resistance, electromagnetic immunity, and long-distance sensing capability. In the past few years, several configurations fiber sensors based on fiber Bragg gratings (FBGs) [1–6] and long period fiber gratings (LPFGs) [7–13] have been developed to measure RI and temperature. The grating-based sensors for the simultaneous measurement of RI and temperature have a serious limitation due to the intrinsic cross-sensitivity of FBGs [2] and need the expensive fabrication equipment (including laser source and phase mask) to make the grating.

In recent years, numerous configurations of all-fiber interferometers have been proposed, such as in-fiber interferometers based on tapered fiber [14], core-offset joint [15,16], two peanut-shape structures [17,18], fiber core diameter mismatch [19,20] and asymmetric structures Mach–Zehnder interferometer [21]. They have something in common is that they only pay considerable attention to the interference between the core mode and the major cladding mode and ignore the interference between the core mode and the other cladding mode. Actually, different order cladding mode will be excited and contribute to the interference pattern. As a result, the different wavelength dips have different response on the ambient RI and temperature. So the simultaneous measurement of RI and temperature can be achieved by monitoring the shift of different wavelength dips simultaneously. The fiber core diameter mismatch has been used for the single parameter measurement of the ambient RI or temperature [19,22]. In this letter, we presented a novel MZI fiber-optical sensor combining the SMS structure and the peanut-shape structure for the simultaneous measurement of the ambient RI and temperature. Compared with the other fiber modal interferometer in Ref. [23], the sensor proposed in this paper has the advantages of high sensitivity due to the high-order cladding modes interference, excellent linearity, more robust and easy fabrication.

2. Sensing principle

The schematic diagram of the sensor is shown in Fig. 1, which is fabricated by a SMS structure cascade with a peanut-shape structure. The multimode fiber (MMF) and the peanut-shape structure act as the mode splitting and combining due to the core

* Corresponding author.
E-mail address: hymeng@scnu.edu.cn (H. Meng).

http://dx.doi.org/10.1016/j.optcom.2015.11.015
0030-4018/

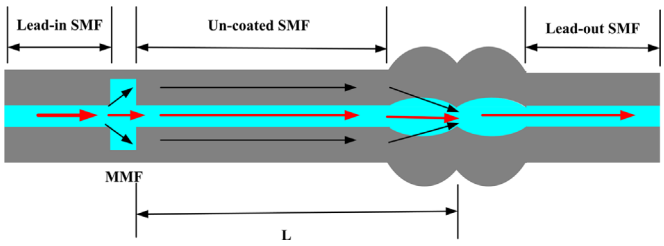

Fig. 1. Schematic diagram of the sensor.

diameter mismatch, respectively. The light from the broadband light source (BBS) is launched into the MMF through the lead-in single mode fiber (SMF). As a result, multiple modes are excited and the field is extended to a larger diameter. The core mode and the cladding modes will propagate in the core and the cladding of the un-coated SMF, respectively. Due to the difference of refractive index between the core and cladding, the core mode and the cladding modes will interfere in the peanut-shape structure and re-couple into the lead-out SMF.

After propagating along the un-coated SMF, the phase difference between the core and cladding modes can be written as [17]

$$\Phi^m = \frac{2\pi\Delta n_{eff}^m L}{\lambda} \tag{1}$$

where the L is the length of the un-coated SMF, Δn_{eff}^m is the effective RI difference between the core mode and the mth cladding mode and λ is the input light wavelength. When the Φ^m in (1) equals $(2N+1)\pi$, the wavelength of the mth attenuation dip can be expressed as [24]

$$\lambda_m = \frac{2\Delta n_{eff}^k L}{2m+1}, \quad m = 1, 2, 3..... \tag{2}$$

We suppose that the difference of the effective index between the core mode and mth cladding mode Δn_{eff}^m changes by δn_{eff}, the mth attenuation peak wavelength will be changed by

$$\delta\lambda_N = \frac{2(\Delta n_{eff}^m + \delta n_{eff})L}{2N+1} - \frac{2\Delta n_{eff}^m L}{2N+1} = \frac{2\delta n_{eff} L}{2N+1} \tag{3}$$

As the ambient RI of the un-coated SMF increasing, the effective RI of the cladding mode will increase and the effective RI of the core mode almost unchanged. As a result, the difference of the effective refractive indices between the core mode and the cladding modes will decrease and the attenuation dips wavelength of the interference spectrum will appear blue-shift. Likewise, as the temperature around the un-coated SMF rising, the effective refractive indices of the core mode and the cladding modes will increase. But, the effect refractive index of the core mode fast increases since thermo-optic coefficient of the fiber core is higher than that of the cladding of fiber. As a result, the attenuation dips wavelength of the interference spectrum will appear red-shift. It is worth to note that the interference spectrum is primarily formed by the interference between the core mode and the dominant cladding mode. But the weak cladding mode also will be excited and the interference between them and the core mode will modulate the main interference pattern. Because of the different cladding modes having different response to the variation of ambient, different transmission dips of the interference spectrum will have different response on the ambient medium parameters. Therefore, the refractive index and temperature can be simultaneously measured by monitoring the shift of two particular transmission dips.

3. Experimental results and discussion

The sensor shown in Fig. 1 was fabricated by splicing two MMFs among three SMFs. A built in fusion mode of SM-MM in the splicer (FITEL S178) was selected, and the arc power and duration were set as 142 bit and 3000 ms, respectively. The core/cladding diameters of the SMF and MMF are 9/125 μm and 105/125 μm, respectively. The length of the MMF has an impact on the interference spectrum because it determines the mode coupling coefficient when the light in the lead-in SMF couples into the un-coated SMF [25,26]. A relatively high coupling coefficient for a particular cladding mode can be achieved by properly choosing the length of the MMF [2,27]. Besides, the length of the MMF should be as short as possible so that the phase differences between the guided modes are negligible. The interference between higher order modes of the MMF should have very large free spectral range (FSR) and therefore the interference patterns might not fall into the measured wavelength region. In the experiment, 3 mm length of the two MMFs was chosen to ensure a good core-cladding coupling, low intensity loss and compact size. It should be pointed out that the length of the un-coated SMF has an impact on the FSR and the sensitivity of the sensor also. In general, with the longer the length of the un-coated SMF, the narrower the FSR of the transmission spectrum and the higher the sensitivity of the sensor can be achieved [20]. In this paper, a 30 mm long un-coated SMF was chosen to ensure a compact size.

A schematic diagram showing the experiment system is depicted in Fig. 2. The light from a broadband source was injected into the structure and the transmission spectrum was recorded by an optical spectrum analyzer (OSA) with a resolution of 0.05 nm.

Fig. 3 shows the transmission spectrum of the sensor when it is immersed in the distilled water at the room temperature. As we can see that the maximum extinction ratio is more than 25 dB and the interference pattern is inhomogeneous. The inhomogeneous characteristics indicated that more than one cladding modes were excited and interfered in the un-coated SMF [28]. In order to get the detail information about the amount of the excited cladding modes, the transmission spectrum shown in Fig. 3 was Fourier transformed to gain the spatial frequency, shown in Fig. 4. From the Fig. 4, there are over six modes are excited, including one domain mode and several weak modes. It should be noted that the different transmission dips have different sensitivities because of different cladding modes interfere with the core mode. In the experiment, we selected the two transmission dips A and B with the wavelength of 1546.50 nm and 1574.36 nm in Fig. 3 to achieve the simultaneous measurement of RI and temperature.

The response of the sensor on ambient RI is investigated by immersing it into NaCl solution with different concentrations at the room temperature. The RI of the NaCl–water solution was calculated with Ref. [27]. After every measurement, the sensor head is cleaned with the distilled water and then is dried until the spectrum comes back to its original shape in air. Fig. 5 shows the wavelength of the transmission dip A and dip B as the ambient RI decreases from 1.3105 to 1.3517. It is clear that the wavelength of two dips experience blue-shift as the ambient RI increases. The shift of dip A and B is −1.13 nm and −3.47 nm in the measurement range, respectively. The corresponding RI sensitivities of dip A and dip B are $K_{A,RI} = -26.5579$ nm/RIU and $K_{B,RI} = -86.7434$ nm/

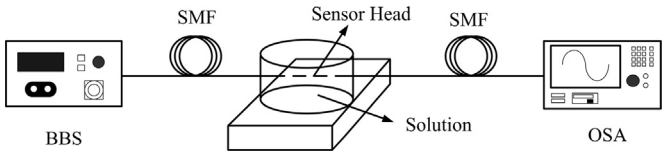

Fig. 2. Schematic diagram of the experiment facility.